Research Article

Journal of PeptideScience

Received: 3 July 2011 Revised: 19 January 2012 Accepted: 20 January 2012 Published online in Wiley Online Library: 20 April 2012

(wileyonlinelibrary.com) DOI 10.1002/psc.2404

Interaction structure of the complex between neuroprotective factor humanin and Alzheimer's β-amyloid peptide revealed by affinity mass spectrometry and molecular modeling

Madalina Maftei,[a] Xiaodan Tian,[a,b] Marilena Manea,[a,c] Thomas E. Exner,[d] Daniel Schwanzar,[e] Christine A. F. von Arnim[e] and Michael Przybylski[a]*

Humanin (HN) is a linear 24-aa peptide recently detected in human Alzheimer's disease (AD) brain. HN specifically inhibits neuronal cell death *in vitro* induced by ß-amyloid (Aß) peptides and by amyloid precursor protein and its gene mutations in familial AD, thereby representing a potential therapeutic lead structure for AD; however, its molecular mechanism of action is not well understood. We report here the identification of the binding epitopes between HN and Aß(1–40) and characterization of the interaction structure through a molecular modeling study. Wild-type HN and HN-sequence mutations were synthesized by SPPS and the HPLC-purified peptides characterized by MALDI-MS. The interaction epitopes between HN and Aß(1–40) were identified by affinity-MS using proteolytic epitope excision and extraction, followed by elution and mass spectrometric characterization of the affinity-bound peptides. The affinity-MS analyses revealed HN(5–15) as the epitope sequence of HN, whereas Aß(17–28) was identified as the Aß interaction epitope. The epitopes and binding sites were ascertained by ELISA of the complex of HN peptides with immobilized Aß(1–40) and by ELISA with Aß(1–40) and Aß-partial sequences as ligands to immobilized HN. The specificity and affinity of the HN-Aß interaction were characterized by direct ESI-MS of the HN-Aß(1–40) complex and by bioaffinity analysis using a surface acoustic wave biosensor, providing a K_D of the complex of 610 nM. A molecular dynamics simulation of the HN-Aß(1–40) complex was consistent with the binding specificity and shielding effects of the HN and Aß interaction epitopes. These results indicate a specific strong association of HN and Aß(1–40) polypeptide and provide a molecular basis for understanding the neuroprotective function of HN. Copyright © 2012 European Peptide Society and John Wiley & Sons, Ltd.

Supporting information can be found in the online version of this article.

Keywords: Alzheimer's disease; neuroprotective peptides; humanin; humanin-ß-amyloid peptide interaction; proteolytic epitope excision and extraction; mass spectrometry; SAW biosensor; ELISA; molecular modeling; confocal laser scanning microscopy

Introduction

AD is the most common form of progressive senile dementia, characterized by memory impairment, disordered cognitive function and decline in language function. AD, which affects more than 25 million people worldwide, leads to inevitable destruction of neurons and ultimately to death [1]. Despite numerous research, there is still poor understanding of the molecular causes and lack of preventive or curative therapies [2]. One of the neuropathological features of AD is represented by the neuritic plaques in brain, consisting of extracellular Aß aggregates and associated axonal and dendritic injury [3]. The neurotoxic Aß peptides, comprising 39–43 amino acids, are released from APP as a result of proteolytic cleavage [1,4].

The main Aß species found in fibrillar neuritic plaques is Aß(1–42), which has a high aggregation propensity, whereas Aß(1–40) is more abundantly produced in cells and is colocalized with Aß(1–42) in plaques [2]. Aß may damage nerve cells through multiple pathways: (i) disruption of calcium regulation leading to cell death; (ii) damage of mitochondria with

* *Correspondence to: Michael Przybylski, Department of Chemistry, University of Konstanz, 78457 Konstanz. E-mail: michael.przybylski@uni-konstanz.de*

a *Laboratory of Analytical Chemistry and Biopolymer Structure Analysis, Department of Chemistry, University of Konstanz, 78457, Konstanz, Germany*

b *Agilent Technologies, 12312, Waldbronn, Karlsruhe, Germany*

c *Zukunftskolleg, University of Konstanz, 78457, Konstanz, Germany*

d *Laboratory of Computational and Theoretical Chemistry, Department of Chemistry, University of Konstanz, 78457, Konstanz, Germany*

e *Department of Experimental Neurology, IZKF Ulm, University of Ulm, 89081, Ulm, Germany*

***Abbreviations used**: AD, Alzheimer's disease; HN, humanin; Aß, ß-amyloid; APP, amyloid precursor protein; FTICR, Fourier transform ion cyclotron resonance; SAW, surface acoustic wave; HRP, horseradish peroxidase; ACN, acetonitrile; NHS, N-hydroxysuccinimide; MD, molecular dynamics; MAP2, microtubule-associated protein 2; FRET, Förster resonance energy transfer; DIV, days in vitro.*

subsequent release of oxygen radicals; and (iii) release of cellular compounds that engender an inflammatory response [5]. The present data suggest that Aß plays a key role in the pathogenesis of AD. Therefore, preventing Aß formation and accumulation or stimulating its clearance represents an important target for therapeutic intervention.

HN is a linear 24-aa peptide cloned from the intact occipital region of an AD brain [6]. HN has been shown to prevent the neuronal cell death *in vitro* caused by Aß and familial AD-related genetic mutations of APP [7]. Recent *in vivo* studies revealed that HN peptides prevent Aß-induced memory impairment in AD mouse models [8]. With the use of immunoblotting with anti-HN antibodies, expression of HN in different mouse organs could be shown [9]. HN immunoreactivity was also detected in human AD brain, but only in traces in an age-matched control brain [9]. The structure–function relationship for the neuroprotective action of HN has been investigated *in vitro* on primary neuronal cultures. N-terminal and C-terminal deletion studies and Ala-scan mutations suggested (Pro3–Pro19) as an essential region for HN activity (Figure 1). Moreover, Cys8Ala mutant (HNA) was inactive, whereas Ser14Gly mutant (HNG) displayed a 1000-fold increase in neuroprotective efficacy compared with wild-type (wt) HN [10].

HN has been shown to be a secretory peptide with a putative binding site on the neuronal cell surface, as suggested by cross-linking experiments with radiolabeled HN [7]. A number of studies focused on identifying the HN receptor, as well as other possible HN-binding partners that mediate its anti-apoptotic activity. Evidence has been obtained that HN participates in STAT3 (signal transducer and activator of transcription 3) factor regulation through a tyrosine kinase pathway [5], whereas other studies indicated intracellular binding partners such as apoptosis-inducing protein Bax [11] and insulin-like growth factor-binding protein 3 [12]. Although HN does not affect the release of Aß peptides from APP [10], it has been efficient against different pathways of Aß neurotoxicity [13,14]. Zou *et al.* [14] showed that HN peptides change the Aß morphology from fibrillary to amorphous and another study reports that HN reduces Aß aggregation by suppressing its effect on mononuclear phagocytes [15]. These findings prompted our interest to study the molecular interaction between HN and Aß(1–40), which may be of relevance for the development of AD-specific therapeutics.

For the identification of peptide and protein interaction structures, affinity-MS in combination with selective proteolytic digestion (epitope excision) and affinity selection of proteolytic fragments (epitope extraction) has been developed and effectively applied in a number of previous studies [16–21]. Here, we report the identification of the interaction epitopes and binding affinity of the complex between HN and Aß(1–40) using affinity-MS, biosensor analysis and ELISA and perform a structural characterization of the complex using molecular docking simulation. The results of this study should contribute to clarify the molecular mechanism of neuroprotection by HN against Aß neurotoxicity.

MAPRG^{5}FSCLL^{10}LLTSE^{15}IDLPV^{20}KRRA

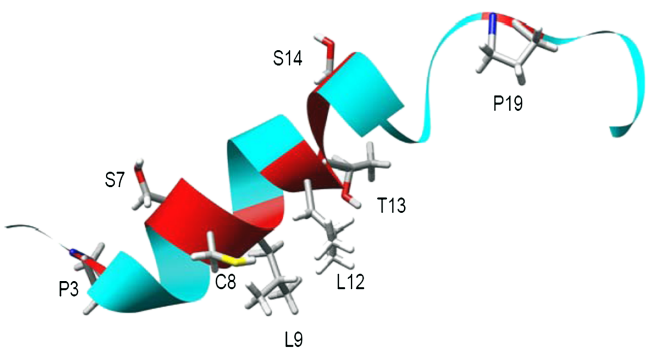

Figure 1. Amino acid sequence and ribbon representation of the structure of HN (PDB file 1Y32). The essential residues for the *in vitro* neuroprotection by HN according to Ala-scan data [10] are marked in red.

Materials and Methods

Synthesis and Purification of HN and Aß Peptides

All peptides were synthesized as carboxyamides on NovaSyn® TGR resin (Novabiochem, Merck KGaA, Darmstadt, Germany) (0.29 mmol/g coupling capacity), using a semi-automated peptide synthesizer (EPS-221, Intavis, Germany) and Fmoc/tBu chemistry. PyBOP and NMM were used as coupling reagents. N-terminal Fmoc protecting groups were removed with 2% piperidine 2% DBU in DMF (2 times 10 min), and each PyBOP-activated amino acid was coupled twice (50 min/coupling). The biotinylated peptides were synthesized with an N-terminal penta-Gly spacer. (Table 1 and Table S1, Supporting Information). In the case of HN peptides, the remaining free amino groups after each second coupling were acetylated using acetic anhydride/NMM/DMF (1.4/1/1.6, v/v/v, 30 min). Cleavage of the peptides from the resin and simultaneous side chain deprotection [except Cys-acetamidomethyl (Acm)] was performed with a mixture of 95% TFA, 2.5% triisopropylsilane and 2.5% H_2O for 3 h. Following precipitation at −20 °C in *tert*-butylmethylether or diethylether, peptides were separated from the resin by vacuum filtration and lyophilized.

Crude peptides were purified by RP-HPLC on a semipreparative C_8 column (HN peptides and Aß(1–16)) or a preparative/semipreparative C_4 column (other Aß sequences). Binary gradients of 0.1% aqueous TFA (eluent A) and 0.1% TFA 80% ACN in H_2O (eluent B) were applied and chromatograms were recorded at detector wavelengths of 220 nm or 214 nm. All peptides were characterized by MALDI-TOF and MALDI-FTICR MS. Analytical data of the synthesized peptides are included in Table 1 and Table S1.

Preparation of Affinity Columns and Affinity-MS

An aliquot of 100 µl HN in H_2O (1 µg/µl) was mixed with 200 µl coupling buffer (100 mM HEPES (4-(2-hydroxyethyl)-1-piperazineethanesulfonic acid), 0.5 M NaCl, pH 7.4) and added to 66.6 mg CH-Sepharose 4B (Sigma-Aldrich, Germany). After 2 h reaction at 20 °C under vigorous shaking, the mixture was transferred into a microcolumn (MoBiTec, Germany) and washed with 10 ml blocking buffer (0.5 M ethanolamine, 0.5 M NaCl, pH 8.3), 10 ml washing buffer (0.2 M CH_3COONa, 0.5 M NaCl, pH 4) and again with 10 ml of the first solution. To block unreacted active groups, the affinity gel was kept in blocking buffer for 1 h at 20 °C; afterwards the washing steps with alternating pH were repeated. Hydrophobically retained molecules were removed by passing through the column 2 ml 6 M guanidine hydrochloride in H_2O, 5 ml phosphate buffered saline (PBS) (6.46 mM $Na_2HPO_4 \times 2H_2O$, 1.47 mM KH_2PO_4, 137 mM NaCl, 2.68 mM KCl, pH 7.4), 2 ml 70% ethanol in H_2O and finally 10 ml PBS. The affinity column was stored in 20% ethanol in H_2O at 4 °C.

In a similar manner, 100 µl Aß(1–40) in TFE (1 µg/µl) was mixed with 200 µl coupling buffer (0.2 M $NaHCO_3$, 0.5 M NaCl, pH 8) and allowed to react with 66.6 mg CH-Sepharose 4B for 2 h at 20 °C.

Journal of PeptideScience

Table 1. Amino acid sequences and structural characterization of synthetic HN peptides

Peptide no.	Code	Sequence	HPLC R_t (min)[a]	$[M+H]^+$ experimental/calculated[b]
1	HN	H-Met-Ala-Pro-Arg-Gly-Phe-Ser-Cys^8-Leu-Leu-Leu-Leu-Thr-Ser^{14}-Glu-Ile-Asp-Leu-Pro-Val-Lys-Arg-Arg-Ala-NH_2	23.32	2687.5/2687.3
2	HN(3–19)	H-Pro-Arg-Gly-Phe-Ser-Cys^8-Leu-Leu-Leu-Leu-Thr-Ser^{14}-Glu-Ile-Asp-Leu-Pro-NH_2	23.55	1873.8/1874.2
3	G_5HN	H-$(Gly)_5$-Met-Ala-Pro-Arg-Gly-Phe-Ser-Cys^8-Leu-Leu-Leu-Leu-Thr-Ser^{14}-Glu-Ile-Asp-Leu-Pro-Val-Lys-Arg-Arg-Ala-NH_2	24.73	2972.4/2972.5
4	BG_5HN	Biotin-$(Gly)_5$-Met-Ala-Pro-Arg-Gly-Phe-Ser-Cys^8-Leu-Leu-Leu-Leu-Thr-Ser^{14}-Glu-Ile-Asp-Leu-Pro-Val-Lys-Arg-Arg-Ala-NH_2	25.83	3198.8/3198.8
5	BG_5HNA	Biotin-$(Gly)_5$-Met-Ala-Pro-Arg-Gly-Phe-Ser-**Ala**^{8}-Leu-Leu-Leu-Leu-Thr-Ser^{14}-Glu-Ile-Asp-Leu-Pro-Val-Lys-Arg-Arg-Ala-NH_2	26.24	3166.7/3166.8
6	BG_5HNG	Biotin-$(Gly)_5$-Met-Ala-Pro-Arg-Gly-Phe-Ser-Cys^8-Leu-Leu-Leu-Leu-Thr-**Gly**^{14}-Glu-Ile-Asp-Leu-Pro-Val-Lys-Arg-Arg-Ala-NH_2	25.97	3168.8/3168.8
7	BG_5HN_{Acm}	Biotin-$(Gly)_5$-Met-Ala-Pro-Arg-Gly-Phe-Ser-**Cys^8(Acm)**-Leu-Leu-Leu-Leu-Thr-Ser^{14}-Glu-Ile-Asp-Leu-Pro-Val-Lys-Arg-Arg-Ala-NH_2	24.98	3269.6/3269.9
8	BG_5HNS	Biotin-$(Gly)_5$-Met-Ala-Pro-Arg-Gly-Phe-Ser-**Ser**^{8}-Leu-Leu-Leu-Leu-Thr-Ser^{14}-Glu-Ile-Asp-Leu-Pro-Val-Lys-Arg-Arg-Ala-NH_2	23.98	3182.7/3182.8

[a]RP-HPLC column: Vydac C_8 (Grace Davison Discovery Science, Deerfield, IL, USA); flow rate: 1 ml/min; gradient: 30–60% B in 30 min.
[b]MALDI-TOF MS.

Blocking and washing of the affinity gel were performed as described previously.

For affinity-MS, a mixture of 9 µg HN and 5.6 µg neurotensin was dissolved in PBS (pH 7.4) and added to the Aß(1–40) affinity column. After 2 h incubation at 20 °C under gentle shaking, the unbound material was removed by washing with 60 ml PBS and elution of the affinity-bound peptide was performed with 2×500 µl 0.1% aqueous TFA (15 min each). After lyophilization and Zip-Tip® (Millipore, Billerica, MA, USA) desalting, supernatant and elution fractions were analyzed by MALDI-MS. A similar protocol was applied to investigate the affinity of HN(3–19) extended epitope to Aß(1–40), with the only differences that 10 µg of synthetic HN(3–19) were used and the supernatant and elution fractions were analyzed by ESI-LC MS.

Bioaffinity Determinations using a Surface Acoustic Wave Biosensor

The S-sens K5 Biosensor instrument (SAW Instruments, Bonn, Germany) is a chip-based system for detection of affinity interactions based on the conversion of a high frequency signal into a SAW, through an inverse piezoelectric effect [22,23]. The velocity of the SAW is affected by changes in mass loading and viscosity caused by molecular interactions on the gold chip surface, which are analyzed as shifts in signal phase and amplitude, respectively. The gold chip surface was covered with a self-assembled monolayer by incubation with 10 mM 16-mercaptohexadecanoic acid in chloroform for 12 h at 20 °C. After washing the chip with chloroform and ethanol, the self-assembled monolayer carboxyl groups were activated by using 50 mM NHS and 200 mM EDC (1 : 1 v/v) in PBS (5 mM $Na_2HPO_4 \times 2H_2O$, 150 mM NaCl, pH 7.4). Two injections of 10 µM Aß(1–40) in PBS (150 µl each) were performed to immobilize the peptide; unreacted active groups were deactivated with 1 M ethanolamine, 0.5 M NaCl (pH 8.3) and unspecific binding sites blocked with a 150 µl injection of 10 µM neurotensin in PBS.

The kinetics of the HN–Aß(1–40) interaction was determined by injecting dilutions of biotinylated HN peptides (0.3–10 µM) in PBS at a flow rate of 20 µl/min, with regeneration of the surface after each binding with 150 µl ACN : 0.1% aqueous TFA (2 : 1). The binding and dissociation curves generated at different ligand concentrations were fitted according to the '1 : 1 binding and residue' model using the OriginPro 7.5 (OriginLab Corp., Northampton, MA, USA) and FitMaster software (SAW Instruments). The observed association rate constants k_{obs} for the five channels were averaged for each dilution, plotted against the analyte concentration and linear regression was applied. The equilibrium dissociation constant (K_D) was obtained according to the following equation:

$$K_D = k_{off} k_{on}^{-1},$$

where k_{off} [s^{-1}] is the dissociation rate constant representing the intersection of the fitted line with the *y*-axis and k_{on} [$conc^{-1}\,s^{-1}$] the association rate constant representing the slope of the linear best fit.

Proteolytic Epitope Excision/Extraction MS

For proteolytic excision experiments, 10 µg Aß(1–40) in PBS (6.46 mM $Na_2HPO_4 \times 2H_2O$, 1.47 mM KH_2PO_4, 137 mM NaCl, 2.68 mM KCl, pH 7.4) were added on the HN affinity column and allowed to bind for 2 h at 20 °C. Excess peptide was washed away

with 60 ml PBS and digestion of the immobilized complex was performed in 250 µl PBS for 2 h at 37 °C, using a protease : peptide (E : S) ratio of 1 : 20 for trypsin (Promega GmbH, Mannheim, Germany), 1 : 40 for Asp-N (Promega GmbH, Mannheim, Germany) and 1 : 50 for chymotrypsin (Sigma-Aldrich Chemie, Munich, Germany). Nonbinding peptide fragments were removed with 60 ml PBS until no MS signal was detectable in the last milliliter of the washing fraction. The remaining affinity-bound peptides were eluted with 2 × 500 µl 0.1% aqueous TFA for 15 min, respectively. In all excision experiments, Sepharose-immobilized HN and Aß(1–40) were found protected from proteolytic cleavage at the applied experimental conditions.

In the proteolytic extraction experiments, 10 µg HN/Aß(1–40) were first digested with trypsin (E : S ratio, 1 : 20) in 250 µl 50 mM NH_4HCO_3 solution (pH 7) for 3 h/4 h at 37 °C or with Glu-C protease (Promega GmbH, Mannheim, Germany) (E : S ratio, 1 : 20) in 250 µl 100 mM NH_4HCO_3 (pH 7) for 36 h/12 h at 37 °C and the resulting peptide mixture was applied onto the HN or Aß(1–40) affinity column, respectively. To protect the affinity gel from enzymatic digestion, 6 µg/ml aprotinin and 15 µg/ml leupeptin were simultaneously added to the column. After removal of unbound fragments with 60 ml PBS, the peptides retained on the column were eluted with 0.1% aqueous TFA.

In all experiments, the supernatant, the final milliliter of the washing fraction and the elution fraction were lyophilized, desalted using Zip-Tip® and analyzed by MALDI-FTICR or MALDI-TOF MS.

Mass Spectrometry

MALDI-TOF MS was performed with a Bruker Biflex™ linear TOF mass spectrometer (Bruker Daltonics, Bremen, Germany) equipped with a nitrogen UV laser (337 nm) and a dual channel plate detector. A saturated solution of α-cyano-4-hydroxy-cinnamic acid in ACN : 0.1% TFA (2 : 1) was used as matrix. Acquisition of spectra was carried out at an acceleration voltage of 20 kV and a detector voltage of 1.5 kV. High resolution FTICR-MS was performed with a Bruker Daltonics Apex II instrument equipped with a 7 T superconducting magnet, a cylindrical infinity ICR analyzer cell and a Scout-100 MALDI or a nano-ESI ion source. A 50 mg/ml solution of 2,4-dihydroxy-benzoic acid in ACN : 0.1% TFA (2 : 1) was used as matrix for MALDI-FTICR MS. For nano-ESI-FTICR MS of the HN-Aß(1–40) complex, 25 µl Aß(1–40) in H_2O (100 µM) were mixed with 12.5 µl BG_5HNA **5** in H_2O (100 µM) and 12.5 µl of 2 mM ammonium acetate (pH 6). The resulting solution (50 µl) contained 2.5 nmol Aß(1–40) (50 µM final concentration) and 1.25 nmol BG_5HNA **5** (25 µM final concentration) in 0.5 mM ammonium acetate (pH 6) and was incubated for 2 h at 20 °C. Nano-ESI-FTICR mass spectra were obtained by accumulation of 15 single scans, with the capillary exit voltage set to 20 V and the skimmer 1 set to 10 V, whereas the capillary voltage was adjusted between −1100 and −1200 V until a stable spray was obtained. The ions were accumulated in the RF-only hexapole for 0.15 s before being transferred into the ICR cell. Calibration, acquisition and processing of spectra were carried out with the Bruker XMASS Software.

ESI-LC MS was carried out using an HP 1100 liquid chromatograph for binary gradient elution and a 150 × 1 mm × 3.5 µm RP-C_8 column (Agilent Technologies, Waldbronn, Germany), coupled to an Esquire 3000 + ion trap mass spectrometer from Bruker Daltonics. The elution system was 0.3% aqueous formic acid (eluent A) and 0.3% formic acid in ACN (eluent B), and a gradient of 20–60% B in 20 min was applied. Ion source parameters were 20 psi nebulizer gas and 9 l/min of drying gas with a temperature of 250 °C.

Enzyme-Linked Immunosorbent Assay

Costar flat bottom 96-well microtiter plates (Biorad, München, Germany) were coated overnight at 4 °C with 100 µl/well Aß(1–40) or $(G)_5HN$ in PBS (6.46 mM $Na_2HPO_4 \times 2H_2O$, 1.47 mM KH_2PO_4, 137 mM NaCl, 2.68 mM KCl, pH 7.4). The peptides were initially dissolved at 0.5 µg/µl in TFE and the necessary amounts diluted with PBS to the coating concentration of 5 µg/ml. After four times washing with 0.1% Tween 20 in PBS (PBST), unspecific binding sites were blocked with 5% BSA in PBST (BSAT) for 2 h at 20 °C. The plates were then washed once with PBST and 1 : 3 dilutions (100 µl/well) of the analyte peptides in BSAT were added and allowed to interact with the binders for 2 h. Ligand peptides were diluted to the working concentrations from stock solutions of 450 µM in H_2O (biotinylated HN peptides) and 100 µM in TFE (biotinylated Aß peptides). The plates were washed five times with Cova Buffer (2 M NaCl, 40 mM $MgSO_4 \times 7\ H_2O$ in PBST) and then incubated for 1 h with HRP-conjugated anti-biotin antibody (Dianova, Germany), diluted 1 : 10 000 in BSAT. Following three washing steps with PBST and one with citrate–phosphate buffer (pH 5), 100 µl 0.1% *o*-phenylenediamine dihydrochloride substrate in citrate–phosphate buffer, containing 0.02 µl 30% H_2O_2, was added to each well. Optical density (OD) was determined at 450 nm on a Wallac 1420 Victor^2 ELISA plate counter.

Molecular Modeling

Theoretical methods based on the Rosetta protein structure prediction and design suite [24,25] were applied for molecular modeling. With the use of the Rosetta ab initio folding protocol, 10 000 structures of the individual peptides were generated and those with an energy score of less than −70 units for Aß(1–40) and less than −33 units for HN were selected. The structures were then clustered by the Rosetta cluster application and the 100 most populated clusters used in the docking studies (297 structures of Aß(1–40) and 513 structures of HN). Docking was carried out with the RosettaDock tool [26]. First, a low-resolution search for each combination of an Aß(1–40) and a HN structure was performed and 100 predictions generated for each pair, resulting in a total of 15 236 100 complexes. Most of these were removed by an energy cutoff of −15 units for the binding energy. The remaining 912 complexes were submitted to the high-resolution search, using a full-atom representation as previously proposed [27], and 100 predictions per input low-resolution structure were obtained. These complexes were further filtered by an energy cutoff of −50 units and clustered. The best structures from the five lowest-energy clusters were selected for subsequent MD calculations. Simulations were carried out with the AMBER 10 program suite (University of California, San Francisco), using the Cornell *et al.* force field [28] (parm99SB) and a periodic water box in the form of a truncated octahedron. After equilibration, production runs of 20 ns were performed in the canonical (NVT) ensemble and the last five were chosen for analysis. The binding energies of the complexes were calculated with the molecular mechanics–generalized Born/surface area (MM-GBSA) method, following the protocol proposed by Gohlke *et al.* [29,30]. To identify the major interactions, the MM-GBSA energy was decomposed into contributions of amino acid pairs [31].

Journal of PeptideScience

Confocal Laser Scanning Microscopy and FRET Analysis (Figures S10 and S11)

Primary hippocampal neurons were dissected from E18 mice, dissociated, plated on glass cover slides in 24-well plates and maintained in Neurobasal medium (Invitrogen, UK) with 1× B-27 serum-free supplement (Invitrogen, UK) and 0.5 mM GlutaMAX (Invitrogen, UK). Neurons (DIV as indicated) were treated with BG_5HNG **6** for 1 h and then fixed with 4% PFA/sucrose (Sigma-Aldrich, Germany) for 15 min, permeabilized with 0.1% saponin (Sigma-Aldrich, Germany) and blocked with 1× ImmunoBlock (Carl Roth, Germany) for 1 h. For dendritic visualization, neurons were stained overnight with chicken anti-MAP2 antibody (EnCor Biotechnology, FL, USA) (1 µg/ml) at 4 °C. Cells were labeled with Alexa-647-conjugated anti-chicken antibody and Alexa-488-conjugated streptavidin (Invitrogen, UK) (1 µg/ml) and imaged by Zeiss LSM 710 with an EC Plan-Neofluar 40×/1.30 oil objective (Zeiss MicroImaging, Germany). Co-occurrence between **6** and the cell surface was correlated by dendritic MAP2 staining with ImageJ (NIH, Bethesda, MD, USA). Intergroup comparisons of colocalization quotient between staining of **6** and dendritic MAP2 staining were performed using Kruskal–Wallis one-way analysis of variance on ranks. To address the problem of multiple comparisons, the test was followed by a post hoc Student–Newman–Keuls test. Data were analyzed using SigmaStat for Windows (Systat Software, IL, USA). Significance was defined as $p < 0.05$ (*).

To analyze the proximity of **6** with APP, Neuro-2A mouse neuroblastoma cells (DSMZ #ACC148) were transfected with APP695 (GenBank #A33292) N-terminally tagged by mRFP (GenBank #AF506027), both having been subcloned by PCR in a CMV-driven empty vector backbone of pEGFP-C1 (GenBank #U55763). The cells were then treated and fixed as described previously and were analyzed using FRET, which is observed when two fluorophores are in close proximity (<10 nm). The donor fluorophore was excited with the Argon laser line 488 nm and the emissions recorded with a 34-channel QUASAR detection unit (Carl Zeiss MicroImaging, Germany).

Results

Specificity and Affinity of the HN–Aß(1–40) Interaction

To evaluate the specificity of the HN interaction with Aß, Aß(1–40) was immobilized to an NHS-activated Sepharose matrix and exposed to an equimolar mixture of HN and neurotensin as a negative control. The MALDI-TOF mass spectrum of the supernatant from the column showed only molecular ions of the control peptide. No ions were detectable in the final washing fraction, whereas the spectrum of the elution fraction contained exclusively the protonated and sodiated singly charged ions of HN (Figure 2A), thus confirming the specificity of the HN–Aß(1–40) interaction.

To ascertain the assumed stoichiometry and presence of a single interaction site, high resolution ESI-FTICR MS was employed for direct molecular characterization of the HN–Aß(1–40) complex. ESI-MS as a 'soft' ionization technique has been applied in the last years in many studies for the characterization of non-covalent biopolymer complexes [32]. A prerequisite for the successful application, however, is the careful optimization of 'native' solution conditions and mass spectrometric parameters, to minimize

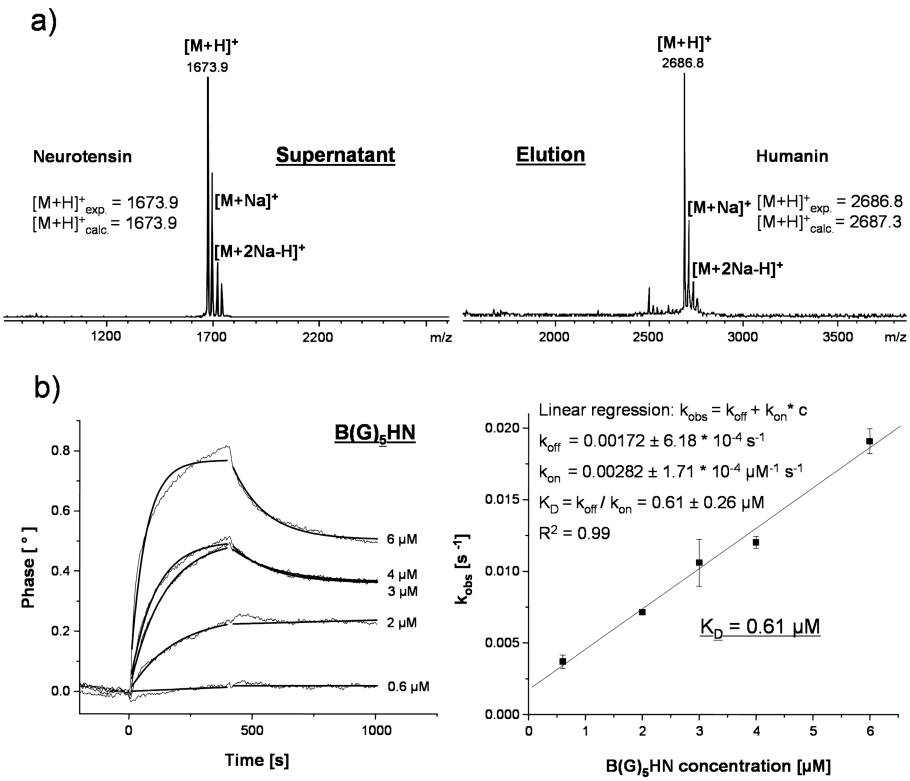

Figure 2. (A) MALDI-TOF affinity mass spectra of HN binding to Sepharose-immobilized Aß(1–40), using neurotensin as a negative control. The supernatant contains only the control peptide, *m/z* 1673.9. HN binds specifically to the Aß(1–40) affinity column, being the only peptide present in the elution fraction (*m/z* 2686.8). (B) Binding and dissociation curves and K_D determination of the complex between BG_5HN and immobilized Aß(1–40).

dissociation of the complex and allow its ionization and transfer into the analyzer cell [33]. The Ala mutant peptide BG_5HNA **5** was used instead of wt HN, because the Cys8Ala replacement provides higher binding affinity to Aß(1–40) (Figure S8a) and prevents possible disulfide bridge formation, which may compete with the formation of the HN–Aß(1–40) complex. In wt HN, we observed a small extent of disulfide dimerization upon incubation of HN in PBS.

Analysis of a dilution series of **5** in 0.5 mM ammonium acetate (pH 6) provided 25 µM as the minimal peptide concentration yielding a good signal to noise ratio in positive ion nano-ESI-FTICR MS. To determine the highest relative amount of the complex, a range of HN peptide **5** : Aß(1–40) concentration ratios was evaluated and revealed a twofold molar excess of the more acidic Aß to be best suited; in contrast, an excess of the more basic HN peptide may suppress ionization of the less basic Aß–HN complex. The nano-ESI-FTICR mass spectrum presented in Figure 3 shows the 5+ charged molecular ion of the 1:1 complex between 5 and Aß(1-40) (*m/z* 1499.18), together with the 3+ and 4+ molecular ions of the free polypeptides. When replacing the ammonium acetate (pH 6) solution with a strongly acidic solution (2% aqueous acetic acid:methanol, 1:1), no complex formation was observed (data not shown), thus confirming the specific interaction between the peptides.

A quantitative determination of the HN–Aß(1–40) interaction was performed by SAW bioaffinity analysis [23], which has been recently emerging as an effective biosensor method and alternative to surface plasmon resonance. Aß(1–40) was immobilized on an NHS-activated gold chip, as described in the Materials and Methods section, and increasing concentrations of wt BG_5HN **4** in PBS were injected. The shifts in the signal's phase, corresponding to different analyte dilutions, were fitted according to a 1 : 1 Langmuir binding model and the calculated rate constants k_{obs} were plotted as a function of the applied concentrations, which provided an equilibrium dissociation constant (K_D) of 0.61 µM (Figure 2B). A similar affinity was obtained for the neuroprotective Ser14Gly mutant BG_5HNG **6** (K_D 0.53 µM). The biosensor quantification results were in good agreement with the ELISA determinations (Figure S8a).

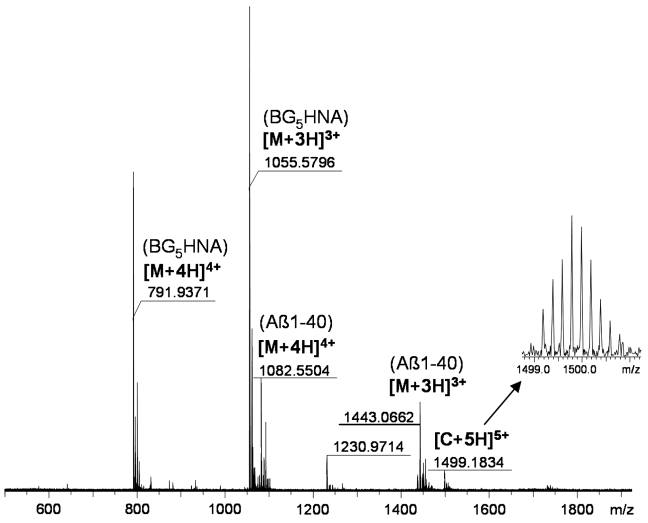

Figure 3. Nano-ESI-FTICR mass spectrum of the 1 : 1 complex of Aß(1–40) (50 µM) and BG_5HNA (25 µM) in 0.5 mM ammonium acetate (pH 6). The isotopic distribution of the (5+) molecular ion of the Aß(1–40)–HN complex is shown in the insert.

Identification of the HN Epitope Recognized by Aß(1–40)

To identify the epitope sequence of HN involved in Aß(1–40) binding, both proteolytic epitope extraction and excision MS were employed, using an Aß(1–40) affinity column and Glu-C, trypsin and chymotrypsin proteases. In a first epitope extraction experiment, HN was digested with Glu-C in solution and the resulting peptide fragment mixture subjected to interaction with Sepharose-immobilized Aß(1–40). The mass spectrometric analysis revealed the nonbinding C-terminal fragment HN(16–24) in the supernatant fraction (Figure 4A), whereas in the elution fraction, only the peptide HN(1–15) was found (Figure 4B), indicating the epitope localization within this N-terminal sequence. In a following proteolytic excision experiment, HN was first bound to the Aß(1–40) column and then subjected to tryptic cleavage. MALDI-FTICR MS of the elution fraction (Figure 4C) provided molecular ions $[M+H]^+$ of the HN peptides (5–21), (5–22) and (1–21), covering the amino acid sequence (5–21). This result was confirmed by epitope extraction of HN with trypsin (Figure S1), which showed in the elution fraction the overlapping partial tryptic fragments (5–21), (1–21), (1–22) and (1–23). Combining the results of the proteolytic extraction and excision experiments, the HN epitope could be assigned to HN(5–15). Additional confirmation was provided by an extraction experiment with chymotrypsin, which produced only the supernatant nonbinding HN fragments (1–6), (13–22), (12–22), (13–24), (12–24), (11–24) and (10–24) by cleavage at Leu and Phe residues within the epitope (Figure S2). A summary of the HN epitope fragments found in the elution fractions from the proteolytic experiments with Glu-C protease, trypsin and chymotrypsin is shown in Table S2.

The binding of the HN(5–15) epitope to Aß(1–40) was confirmed by affinity-MS (Figure S3), using the elongated sequence HN(3–19) **2**. This longer epitope peptide was advantageous to avoid solubility problems due to the strong hydrophobicity of HN(5–15). The neuroprotective efficacy of HN(3–19) in neuronal cell lines has been described to be similar to that observed for wt HN [10].

Identification of the Aß(1–40) Epitope Recognized by HN

For the identification of the Aß(1–40) epitope recognized by HN, an identical proteolytic extraction/excision mass spectrometric approach was applied, using a HN affinity column and trypsin, Glu-C, Asp-N and chymotrypsin as proteases. The mass spectrum of the supernatant fraction upon tryptic digestion of Aß in solution and subsequent affinity selection of the proteolytic peptides on Sepharose-immobilized HN revealed the nonbinding fragments Aß(1–16) and Aß(6–16), thus excluding the N-terminal region as part of the epitope (Figure S4). The corresponding elution fraction contained four overlapping peptides covering the sequence Aß(17–28), which was assigned as the binding region to HN (Figure 5A). This epitope was confirmed by proteolytic excision of HN-bound Aß(1–40) with trypsin, which provided only Aß(6–40) and intact Aß(1–40) in the elution fraction, indicating that residues Lys-16 and Lys-28, although accessible for cleavage in solution, were shielded in the HN–Aß(1–40) complex against proteolysis (Figure S5).

Studies using additional proteases produced complementary results to ascertain the Aß epitope. An extraction experiment with Glu-C provided the nonbinding fragments Aß(4–11) and Aß(12–22) in the supernatant fraction, thus excluding the epitope location within these N-terminal sequences (Figure S6a). The corresponding elution fraction contained peptides overlapping Aß(12–40) (Figure S6b). Proteolytic excision of HN-bound Aß with Asp-N protease showed Aß(7–40) as the only epitope fragment in

Journal of PeptideScience

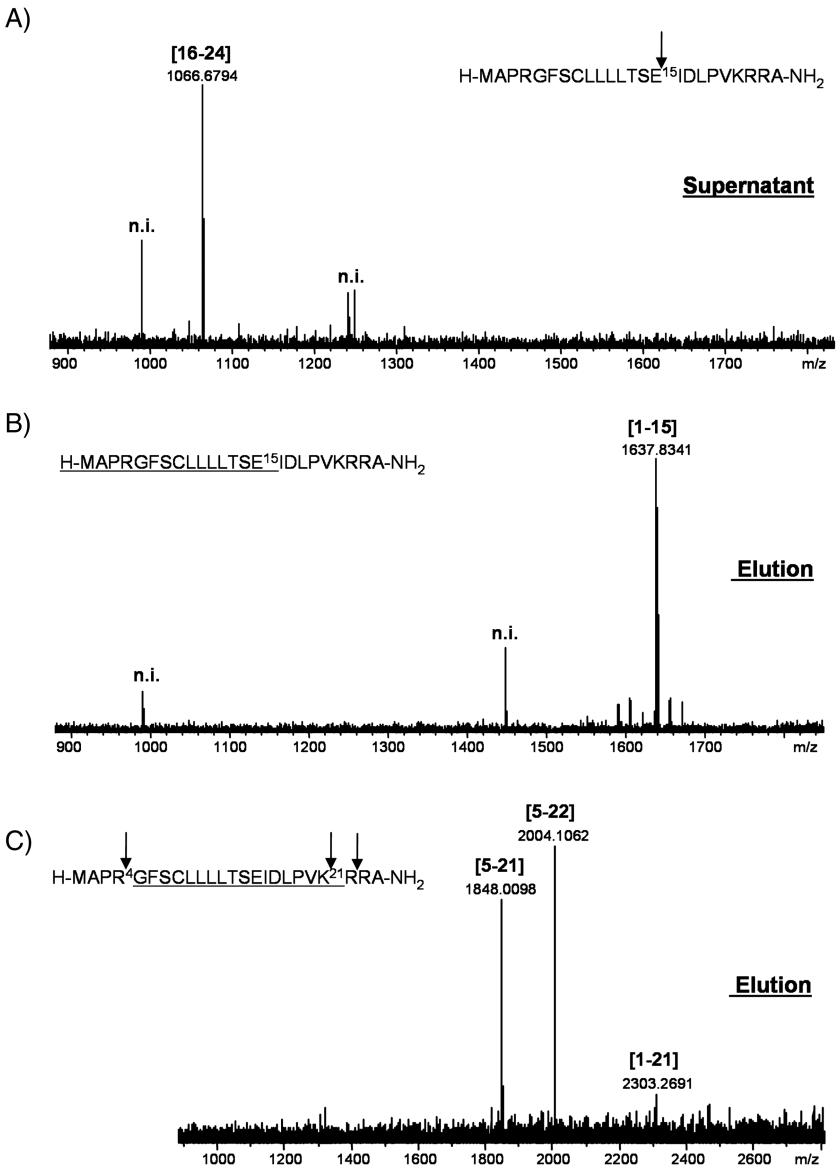

Figure 4. MALDI-FTICR mass spectrum of (A) the supernatant fraction obtained after digestion of HN with Glu-C protease and addition of the fragment mixture on the Aß(1–40) affinity column (proteolytic extraction), showing the nonbinding peptide HN(16–24). The Glu-C cleavage site is indicated by an arrow; n.i. not identified; (B) the elution fraction after proteolytic extraction of HN with Glu-C, showing the binding sequence HN(1–15) (underlined); (C) the elution fraction obtained after proteolytic excision of HN with trypsin. The trypsin cleavage sites are indicated by arrows and the HN(5–21) epitope sequence is underlined.

the elution (Figure 5C). We observed shielding from cleavage at Asp-23, although the residue was accessible for proteolysis in solution (Figure 5B). Further, epitope excision with chymotypsin revealed shielding of Leu-17, Phe-19 and Phe-20 upon HN binding, whereas Phe-4, Tyr-10, His-13 and Ala-30 were amenable to digestion (Figure S7).

The molecular ions found in the elution fractions from all the described proteolytic experiments are summarized in Table S3. Consistent with all proteolytic results, we conclude that HN interacts with the Aß(17–28) sequence. Furthermore, residues Lys-16, Leu-17, Phe-19, Phe-20, Asp-23 and Lys-28 are all protected by HN binding against proteolytic cleavage, suggesting their involvement in the HN–Aß(1–40) complex.

Affinity Characterization of the HN-Aß(1–40) Complex by ELISA

The interaction affinities of wt HN and HN variants to Aß(1–40) were further characterized by ELISA, using HN sequences elongated with a penta-Gly spacer and biotinylated at the N-terminus, to ensure optimal exposure of the HN epitope to Aß(1–40) during incubation and detection with HRP-conjugated anti-biotin antibody (Figure S8a). With the ELISA data, the effect of HN sequence mutations on the Aß(1–40) recognition could be assessed. The Cys8Ala-variant BG_5HNA **5** exhibited the highest affinity to Aß(1–40). The wt peptide BG_5HN **4** and the Ser14Gly-mutant (BG_5HNG, **6**) had similar binding levels to Aß(1–40) as **5** at low concentrations, but showed binding saturation at concentrations $>0.33\ \mu M$. The two HN derivatives in which Cys-8 was either alkylated by Acm (BG_5HN_{Acm} **7**) or substituted with Ser (BG_5HNS **8**) revealed significantly lower affinity to Aß(1–40) than the wt peptide **4**. The data are consistent with Cys-8 and adjacent residues being part of the HN epitope, in agreement with the mass spectrometric data, because replacement of Cys-8 with the more polar Ser residue (peptide **8**) or introduction of the Acm-group in **7** may disturb the mainly hydrophobic interaction structure between HN and Aß.

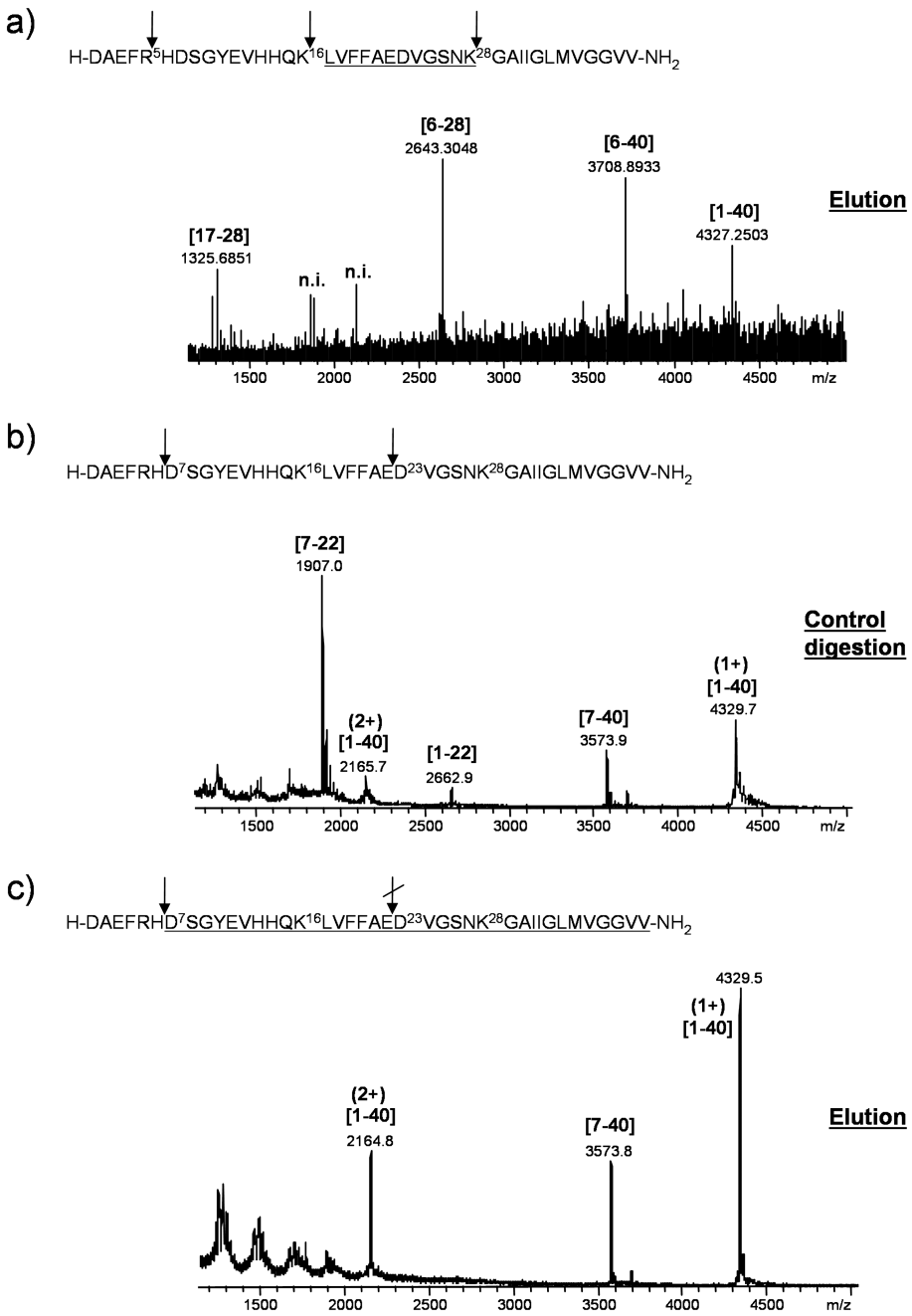

Figure 5. (A) MALDI-FTICR mass spectrum of the elution fraction after addition of trypsin-digested Aß(1–40) on the HN affinity column (proteolytic extraction). The trypsin cleavage sites are indicated by arrows and the minimal epitope sequence Aß(17–28) is underlined; n.i. not identified; (B) MALDI-TOF mass spectrum of the fragment peptides obtained after Asp-N digestion of free Aß(1–40) in solution (control digestion). The Asp-N cleavage sites are indicated by arrows; (C) MALDI-TOF mass spectrum of the elution fraction obtained after proteolytic excision of Aß(1–40) with Asp-N. The Asp-23, shielded from Asp-N digestion in the Aß-HN complex, is indicated by a broken arrow and the Aß(7–40) epitope sequence is underlined.

A similar ELISA approach was applied to assess the affinities of Aß(1–40) and Aß-partial sequences to HN. All Aß peptides comprising the (17–28) epitope bound to HN, consistent with the mass spectrometric results (Figure S8b).

Structure Modeling of the HN–Aß(1–40) Complex

Theoretical methods based on the Rosetta protein structure prediction and design suite [24,25] were used to obtain structural information on the interaction between HN and Aß(1–40). Using the available NMR structures of both peptides (HN–PDB entry 1Y32; Aβ(1–40)-PDB entry 1AML), the RosettaDock tool [26] was employed in a first approach for rigid body positioning of the docking partners and simultaneous optimization of side chain conformations. Of the 10 000 structures thus generated, none showed a reasonable binding energy upon evaluation with Rosetta energy function. A possible explanation is that HN and Aß(1–40), possessing highly flexible structures, adapt to each other upon complex formation; therefore, a prediction model for their association by rigid docking seems unlikely to be successful.

In a second approach, the best structures from the five lowest-energy clusters of the Rosetta calculations were selected for MD

Journal of PeptideScience

simulations. These HN–Aß(1–40) complexes are illustrated in Figure S9 and the corresponding binding energies are shown in Table 2. According to the MD results, hydrogen bonding, hydrophobic and electrostatic interactions take place upon HN–Aß(1–40) association. The most stable complex (Figure 6) showed Phe-6 residue of HN involved in hydrogen bonding with Phe-19 and in a parallel π overlap with Phe-20 of Aß(1–40); Van der Waals contacts are present between Phe-6 of HN and Val-18 of Aß(1–40), as well as between Ser-7 of HN and Leu-17 and Phe-19 residues of Aß(1–40). These interactions are consistent with the shielding effects observed in the proteolytic excision mass spectrometric experiments at residues Lys-16, Leu-17, Phe-19 and Phe-20 of Aß(1–40). They also support the observed differences in Aß(1–40)-binding affinities of the HN mutants containing a modified Cys-8 residue (Figure S8a). The structure model further suggests the formation of a salt bridge between Asp-17 of HN and Lys-28 of Aß(1–40), in agreement with the observed inaccessibility of Lys-28 residue to proteolytic cleavage. In conclusion, the molecular modeling study of the HN–Aß(1–40) complex provided useful complementary information on the relative orientations of the peptides and their interacting structures.

Discussion and Conclusions

HN is a potent neuroprotective peptide expressed in intact areas of human AD brain [9]. In the present study, we have investigated the molecular interaction between HN and Aß(1–40), using a combination of analytical techniques. Affinity-MS and kinetic data showed that HN specifically binds to Aß(1–40) with high affinity (K_D 0.61 μM). Direct analysis of the HN–Aß(1–40) complex by high-resolution FTICR-MS and the ELISA data further ascertained these results. The interacting region of HN with Aß(1–40) was determined by proteolytic extraction and excision MS to be HN (5–15), within the (3–19) 'core' domain comprising the essential residues for *in vitro* neuroprotective effect [10].

For Aß(1–40), the proteolytic extraction/excision mass spectrometric data showed that the HN binding site is located within region (17–28), which is critically important for the aggregation of Aß. Thus, the Aß(12–24) sequence is involved in parallel ß-sheet formation in fibrils [34,35], whereas residues (17–21) generate side chain interactions and dimerization of Aβ [36]. The importance of the Aß(16–22) sequence for assembly has been shown by single site mutations [4,37,38]. Moreover, the sequence Aß(25–35) is essential for oligomerization and fibril formation [39]. Therefore, due to its interaction with residues (17–28) of monomeric Aß(1–40), HN could prevent Aß oligomerization, fibrillization and subsequent toxicity.

First studies have been performed on the possible interaction of HN with the extracellular juxtamembrane Aß(17–28) sequence of the membrane-anchored amyloid precursor protein in neuronal cells. Fluorescence staining indicated a concentration-dependent membrane attachment of synthetic BG_5HNG **6**, correlated with neuronal maturation (Figure S10). Immunofluorescence staining of endogenous APP provided the visualization of the protein expression at an earlier date than the observed HN-membrane binding (Figure S11a), whereas first FRET studies indicated no close proximity yet between BG_5HNG **6** and fluorescence-tagged APP (Figure S11b). The assumed inhibitory action of HN on Aß aggregation, its phospholipid membrane localization and toxic effects in neuronal membranes [40] are subjects of current investigations.

Table 2. Binding energies of the best structures from the five lowest-energy clusters according to the Rosetta scoring function (arbitrary units) and the MM-GBSA approach (kcal/mol)

Energy function	Complex				
	C1	C2	C3	C4	C5
Rosetta	−111.29	−110.55	−110.29	−108.74	−108.28
MM-GBSA	−30.88	−27.98	−29.07	−58.59	−38.11

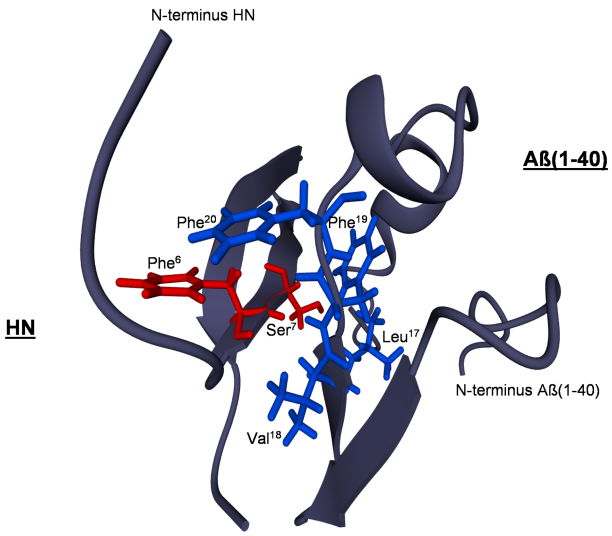

Figure 6. Interaction structure of the HN–Aß(1–40) complex revealed by MD simulation. The binding residues Phe-6 and Ser-7 of the HN peptide are shown in red, whereas the interacting sequence ^{17}LVFF^{20} of Aß(1–40) is represented in blue.

Acknowledgements

This work was supported in part by grants from the Heidelberg Academy of Sciences and Humanities (WIN-Kolleg Junior Academy for Young Scholars and Scientists; to C. A. and M. M.), the Deutsche Forschungsgemeinschaft, Bonn, Germany and the Research Centre Proteostasis, University of Konstanz (to M. P.). We thank the SAW Instruments, Bonn, for the technical support and Mihaela Stumbaum for the expert assistance with the biosensor analyses.

References

1 St George-Hyslop PH. Piecing together Alzheimer's. *Sci. Am.* 2000; **283**: 76–83.
2 Selkoe DJ. Alzheimer's disease: genes, proteins, and therapy. *Physiol. Rev.* 2001; **81**: 741–766.
3 Dickson DW. The pathogenesis of senile plaques. *J. Neuropathol. Exp. Neurol.* 1997; **56**: 321–339.
4 Esler WP, Wolfe MS. A portrait of Alzheimer secretases—new features and familiar faces. *Science* 2001; **293**: 1449–1454.
5 Hashimoto Y, Suzuki H, Aiso S, Niikura T, Nishimoto I, Matsuoka M. Involvement of tyrosine kinases and STAT3 in Humanin-mediated neuroprotection. *Life Sci.* 2005; **77**: 3092–3104.
6 Hashimoto Y, Ito Y, Niikura T, Shao Z, Hata M, Oyama F, Nishimoto I. Mechanisms of neuroprotection by a novel rescue factor humanin from Swedish mutant amyloid precursor protein. *Biochem. Biophys. Res. Commun.* 2001; **283**: 460–468.
7 Hashimoto Y, Niikura T, Tajima H, Yasukawa T, Sudo H, Ito Y, Kita Y, Kawasumi M, Kouyama K, Doyu M, Sobue G, Koide T, Tsuji S, Lang J, Kurokawa K, Nishimoto I. A rescue factor abolishing neuronal cell

death by a wide spectrum of familial Alzheimer's disease genes and Abeta. *Proc. Natl. Acad. Sci. U. S. A.* 2001; **98**: 6336–6341.
8 Kunesova G, Hlavacek J, Patocka J, Evangelou A, Zikos C, Benaki D, Paravatou-Petsotas M, Pelecanou M, Livaniou E, Slaninova J. The multiple T-maze in vivo testing of the neuroprotective effect of humanin analogues. *Peptides* 2008; **29**: 1982–1987.
9 Tajima H, Niikura T, Hashimoto Y, Ito Y, Kita Y, Terashita K, Yamazaki K, Koto A, Aiso S, Nishimoto I. Evidence for in vivo production of Humanin peptide, a neuroprotective factor against Alzheimer's disease-related insults. *Neurosci. Lett.* 2002; **324**: 227–231.
10 Hashimoto Y, Niikura T, Ito Y, Sudo H, Hata M, Arakawa E, Abe Y, Kita Y, Nishimoto I. Detailed characterization of neuroprotection by a rescue factor humanin against various Alzheimer's disease-relevant insults. *J. Neurosci.* 2001; **21**: 9235–9245.
11 Guo B, Zhai D, Cabezas E, Welsh K, Nouraini S, Satterthwait AC, Reed JC. Humanin peptide suppresses apoptosis by interfering with Bax activation. *Nature* 2003; **423**: 456–461.
12 Ikonen M, Liu B, Hashimoto Y, Ma L, Lee KW, Niikura T, Nishimoto I, Cohen P. Interaction between the Alzheimer's survival peptide humanin and insulin-like growth factor-binding protein 3 regulates cell survival and apoptosis. *Proc. Natl. Acad. Sci. U. S. A.* 2003; **100**: 13042–13047.
13 Kariya S, Takahashi N, Ooba N, Kawahara M, Nakayama H, Ueno S. Humanin inhibits cell death of serum-deprived PC12h cells. *Neuroreport* 2002; **13**: 903–907.
14 Zou P, Ding Y, Sha Y, Hu B, Nie S. Humanin peptides block calcium influx of rat hippocampal neurons by altering fibrogenesis of Abeta (1–40). *Peptides* 2003; **24**: 679–685.
15 Ying G, Iribarren P, Zhou Y, Gong W, Zhang N, Yu ZX, Le Y, Cui Y, Wang JM. Humanin, a newly identified neuroprotective factor, uses the G protein-coupled formylpeptide receptor-like-1 as a functional receptor. *J. Immunol.* 2004; **172**: 7078–7085.
16 Dragusanu M, Petre BA, Przybylski M. Epitope motif of an anti-nitrotyrosine antibody specific for tyrosine-nitrated peptides revealed by a combination of affinity approaches and mass spectrometry. *J. Pept. Sci.* 2011; **17**: 184–191.
17 Juszczyk P, Paraschiv G, Szymanska A, Kolodziejczyk AS, Rodziewicz-Motowidlo S, Grzonka Z, Przybylski M. Binding epitopes and interaction structure of the neuroprotective protease inhibitor cystatin C with beta-amyloid revealed by proteolytic excision mass spectrometry and molecular docking simulation. *J. Med. Chem.* 2009; **52**: 2420–2428.
18 Stefanescu R, Born R, Moise A, Ernst B, Przybylski M. Epitope structure of the carbohydrate recognition domain of asialoglycoprotein receptor to a monoclonal antibody revealed by high-resolution proteolytic excision mass spectrometry. *J. Am. Soc. Mass Spectrom.* 2011; **22**: 148–157.
19 Stefanescu R, Iacob RE, Damoc EN, Marquardt A, Amstalden E, Manea M, Perdivara I, Maftei M, Paraschiv G, Przybylski M. Mass spectrometric approaches for elucidation of antigenantibody recognition structures in molecular immunology. *Eur J Mass Spectrom* (Chichester, Eng) 2007; **13**: 69–75.
20 Suckau D, Kohl J, Karwath G, Schneider K, Casaretto M, Bitter-Suermann D, Przybylski M. Molecular epitope identification by limited proteolysis of an immobilized antigen-antibody complex and mass spectrometric peptide mapping. *Proc. Natl. Acad. Sci. U. S. A.* 1990; **87**: 9848–9852.
21 Tian X, Maftei M, Kohlmann M, Allinquant B, Przybylski M. Differential epitope identification of antibodies against intracellular domains of Alzheimer's amyloid precursor protein using high resolution affinity-mass spectrometry. *Subcell. Biochem.* 2007; **43**: 339–354.
22 Andra J, Bohling A, Gronewold TM, Schlecht U, Perpeet M, Gutsmann T. Surface acoustic wave biosensor as a tool to study the interaction of antimicrobial peptides with phospholipid and lipopolysaccharide model membranes. *Langmuir* 2008; **24**: 9148–9153.
23 Gronewold TM. Surface acoustic wave sensors in the bioanalytical field: recent trends and challenges. *Anal. Chim. Acta* 2007; **603**: 119–128.
24 Bonneau R, Strauss CE, Rohl CA, Chivian D, Bradley P, Malmstrom L, Robertson T, Baker D. De novo prediction of three-dimensional structures for major protein families. *J. Mol. Biol.* 2002; **322**: 65–78.
25 Bradley P, Chivian D, Meiler J, Misura KM, Rohl CA, Schief WR, Wedemeyer WJ, Schueler-Furman O, Murphy P, Schonbrun J, Strauss CE, Baker D. Rosetta predictions in CASP5: successes, failures, and prospects for complete automation. *Proteins* 2003; **53**(Suppl 6): 457–468.
26 Kortemme T, Baker D. A simple physical model for binding energy hot spots in protein–protein complexes. *Proc. Natl. Acad. Sci. U. S. A.* 2002; **99**: 14116–14121.
27 Gray JJ, Moughon S, Wang C, Schueler-Furman O, Kuhlman B, Rohl CA, Baker D. Protein–protein docking with simultaneous optimization of rigid-body displacement and side-chain conformations. *J. Mol. Biol.* 2003; **331**: 281–299.
28 Cornell WD CC, Bayly IR, Gould IR, Merz KM, Ferguson DM, Spellmeyer DC, Fox T, Caldwell JW, Kollman PA. A second generation force field for the simulation of proteins, nucleic acids, and organic molecules. *J. Am. Chem. Soc.* 1995; **117**: 5179–5197.
29 Gohlke H, Case DA. Converging free energy estimates: MM-PB(GB)SA studies on the protein–protein complex Ras–Raf. *J. Comput. Chem.* 2004; **25**: 238–250.
30 Gohlke H, Kiel C, Case DA. Insights into protein–protein binding by binding free energy calculation and free energy decomposition for the Ras–Raf and Ras–RalGDS complexes. *J. Mol. Biol.* 2003; **330**: 891–913.
31 Gohlke H, Kuhn LA, Case DA. Change in protein flexibility upon complex formation: analysis of Ras-Raf using molecular dynamics and a molecular framework approach. *Proteins* 2004; **56**: 322–337.
32 Loo JA. Studying noncovalent protein complexes by electrospray ionization mass spectrometry. *Mass Spectrom. Rev.* 1997; **16**: 1–23.
33 Benkestock K, Sundqvist G, Edlund PO, Roeraade J. Influence of droplet size, capillary-cone distance and selected instrumental parameters for the analysis of noncovalent protein-ligand complexes by nano-electrospray ionization mass spectrometry. *J. Mass Spectrom.* 2004; **39**: 1059–1067.
34 Petkova AT, Ishii Y, Balbach JJ, Antzutkin ON, Leapman RD, Delaglio F, Tycko R. A structural model for Alzheimer's beta -amyloid fibrils based on experimental constraints from solid state NMR. *Proc. Natl. Acad. Sci. U. S. A.* 2002; **99**: 16742–16747.
35 Tycko R. Insights into the amyloid folding problem from solid-state NMR. *Biochemistry* 2003; **42**: 3151–3159.
36 Serpell LC, Blake CC, Fraser PE. Molecular structure of a fibrillar Alzheimer's A beta fragment. *Biochemistry* 2000; **39**: 13269–13275.
37 Ghiso J, Frangione B. Amyloidosis and Alzheimer's disease. *Adv. Drug Deliv. Rev.* 2002; **54**: 1539–1551.
38 Miravalle L, Tokuda T, Chiarle R, Giaccone G, Bugiani O, Tagliavini F, Frangione B, Ghiso J. Substitutions at codon 22 of Alzheimer's abeta peptide induce diverse conformational changes and apoptotic effects in human cerebral endothelial cells. *J. Biol. Chem.* 2000; **275**: 27110–27116.
39 Pike CJ, Walencewicz-Wasserman AJ, Kosmoski J, Cribbs DH, Glabe CG, Cotman CW. Structure-activity analyses of beta-amyloid peptides: contributions of the beta 25–35 region to aggregation and neurotoxicity. *J. Neurochem.* 1995; **64**: 253–265.
40 Williams TL, Serpell LC. Membrane and surface interactions of Alzheimer's Aβ peptide-insights into the mechanism of cytotoxicity. *FEBS J.* 2011; **278**: 3905–3917.

